Analysis of the Simulation Fidelity for Extended Target in MMWSS

Jing MA[1], Qiuru HE[1], Duzheng QING[1], Xuguang LUO[1], Congjun JIN[1]

and Dong CHEN[2]

[1]National Key Laboratory of Science and Technology on Missile Control System Simulation
[2]China Academy of Space Technology, Institute of Satellite Telecommunications

Email: Phd.jingma@gmail.com

Abstract

The simulation for Millimeter Wave (MMW) target is that making use of the method of HWIL (Hardware in Loop) to simulate the target and environment signal within the intercepted processing of radar guidance missile in EHF frequency. The target and environment signal simulation in EHF includes two aspects: space property and electromagnetism property. Space property indicates the position of target and the variety of position. Electromagnetism property indicates the amplitude, glint, Doppler shift, distance/angular spread and polarization of echo signal. In MMW target simulation, detection with MMW can improve the distance and angular resolution. One-point target simulation, which views a target as one point scattering, has been testified satisfying the simulation precision in MMWSS. Our intention in this paper is to demonstrate whether the precision of extended target simulation, in which the target is simulated as the aggregation of Scattering Centers (SC) by adjusting amplitudes and phases, can achieve the required precision.

Key Words: Extended Target Simulation, HWIL, Simulation Fidelity

Presenting Author's biography

Jing MA. She received the Bachelor degree in Telecommunications and Ph.D. degree in Signal Processing from Xidian University, China, in 2004 and 2009, respectively. She was a Visiting Student at Microsoft Research Asia in 2006. From 2007 to 2008, she was a Visiting Scholar in the Space Science Engineer Center, University of Wisconsin-Madison, U.S.A.. Since 2009, she has been a Research Engineer for CASIC (China Aerospace Science and Industry Corporation), where her research interests include target and environment Radio Frequency simulation, HWIL(Hardware in Loop) Simulation and VV&A (Verification, Validation and Accreditation) in modeling and simulation.

1 Millimeter Wave Simulation System

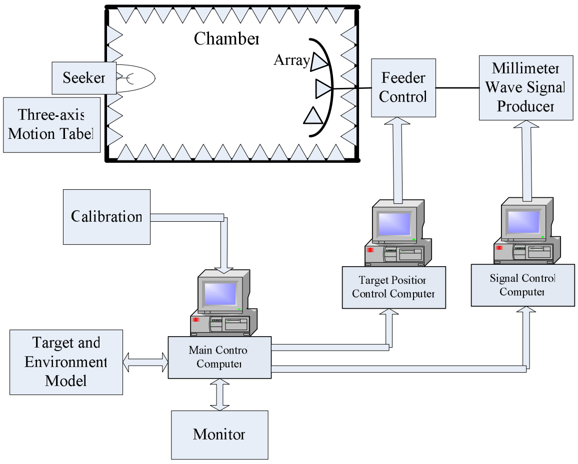

Fig. 1 MMWSS

Millimeter Wave Simulation System (MMWSS), shown as Fig. 1, is composed of chamber, array and feed controller, MMS signal producer, computer and interface, target and environment model, monitor and display system[1]. In the processing of target simulation, the database of target and environment model calculates the space and electromagnetism property of targets. Then the array simulates the electric radiation for seeker detection.

2 The Modeling and Simulation of MMW Extended Target

When the seeker has highly distance resolution, the target is considered as distance extended target because the size of target exceeds the distance resolution of seeker. The target is considered as angular extended target because the angular of target exceeds the angular resolution of the seeker. Usually, the target can be seen as a distance-angular extended one when the seeker owns the power of detection in EHF[2]. The extended target is firstly modeled as geometry model according to its shape. Secondly, the grid model, as Fig. 2 shown, is built by separating the geometry model to grids. In succession, the electromagnetic dispersion model is built based on geometrical optics, geometrical theory of diffraction, physical optics and physical theory of diffraction. Several SC in different units are chosen to represent the extended target. The chosen SC are shown in Fig. 3.

In MMWSS, geometry model, grid model, electromagnetic dispersion model and chosen SC are dealt with the database of target and environment model. Amplitude-phase control strategy is transferred to signal producer system and feed controller. Some Triad of Antennas(TOA) selected in array simulate the electric characters of SC. In the feed circuits, a SC is controlled by one circuit and four circuits consist of one TOA.

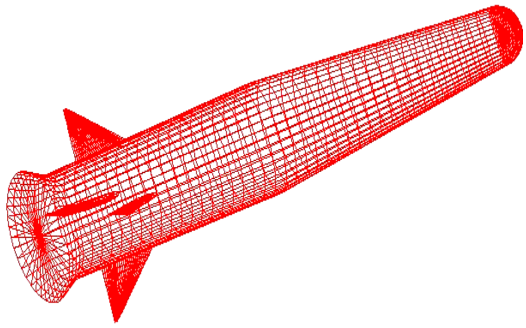

Fig. 2 Grid Mode

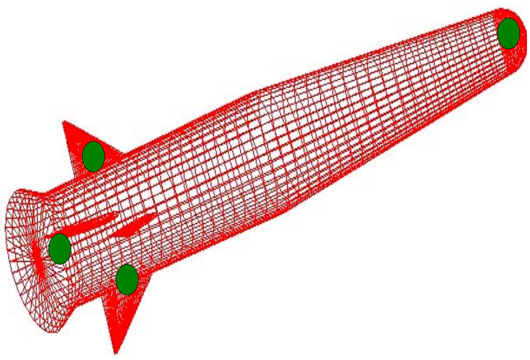

Fig. 3 Scattering Centers Chosen

3 Analysis of the Fidelity of Target Simulation

According to the radar angular measuring principle, the direction of target observed by radar is the gradient direction of the phases wave-front formed by scattering electromagnetic waves on antenna aperture surface[3]. When simulating the echo wave of target with TOA array, the electromagnetic fields generated by each antenna in TOA will be superposed on the receiving antenna aperture surface. In following section, we will discuses whether MMWSS is effective or not in target simulation.

3.1 One-point Target

For radiation-type MMWSS, the size of chamber can meet the far-field radiation conditions for TOA. To simplify the calculation, the curvature of array is not taken into account. So the polarization directions of three antennas of TOA are same. Suppose the electric amplitude on antenna is E_i and the phase is β_i (i=1,2,3), due to each antenna on TOA can be seen as a point. Based on superposition theory, electromagnetic field generated on the receiving antenna aperture surface is

$$E(x,y,z)=\sum_{i=1}^{3}\frac{E_i}{R_i}e^{j\beta_i}e^{-jkR_i} \tag{1}$$

Suppose the polarization direction in (1) is same, the difference on direction of E_1, E_2 and E_3 can be neglected.

Therefore

$$R_i=\sqrt{(x_i-x)^2+(y_i-y)^2+(z_i-z)^2} \tag{2}$$

(x_i, y_i, z_i) is the coordinate for the *i*th antenna on TOA. (x, y, z) is the coordinate on the receiving antenna aperture surface of seeker.

Let

$$A_i=\frac{E_i}{R_i} \tag{3}$$

Superposed electromagnetic field on the aperture surface of seeker is

$$\begin{aligned}E(x,y,z)&=\sum_{i=1}^{3}A_i e^{j(\beta_i-kR_i)}\\&=\sum_{i=1}^{3}A_i\left[\cos(\beta_i-kR_i)+j\sin(\beta_i-kR_i)\right]\\&=\sum_{i=1}^{3}A_i\cos(\beta_i-kR_i)+j\sum_{i=1}^{3}A_i\sin(\beta_i-kR_i)\end{aligned} \tag{4}$$

Then

$$\begin{aligned}&\left|E(x,y,z)\right|\\&=\sqrt{\left[\sum_{i=1}^{3}A_i\cos(\beta_i-kR_i)\right]^2+\left[\sum_{i=1}^{3}A_i\sin(\beta_i-kR_i)\right]^2}\end{aligned} \tag{5}$$

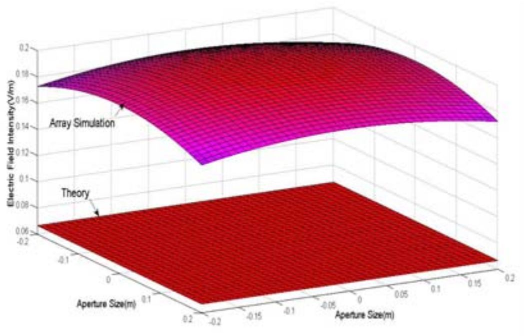

(a) Electric Field Intensity Distribution

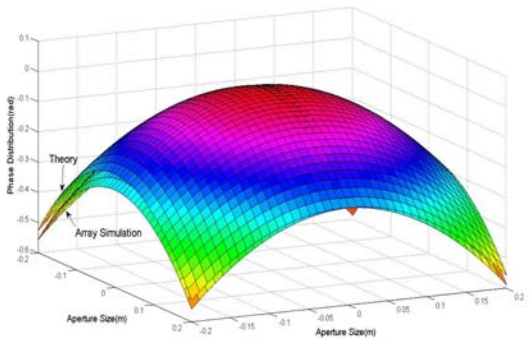

(b) Phase Distribution

Fig. 4 Electromagnetic Fields of TOA and SP

After simplification,

$$\left|E(x,y,z)\right|=\sqrt{A_1^2+A_2^2+A_3^2+2A_1A_2\cos\varphi_{12}+2A_1A_3\cos\varphi_{13}+2A_2A_3\cos\varphi_{23}} \tag{6}$$

$$\beta(x,y,z)=a\tan\left[\frac{A_1\sin(\beta_1-kR_1)+A_2\sin(\beta_2-kR_2)+A_3\sin(\beta_3-kR_3)}{A_1\cos(\beta_1-kR_1)+A_2\cos(\beta_2-kR_2)+A_3\cos(\beta_3-kR_3)}\right] \tag{7}$$

where

$$\varphi_{12} = (\beta_2 - \beta_1) - k(R_2 - R_1)\,,$$
$$\varphi_{13} = (\beta_3 - \beta_1) - k(R_3 - R_1)\,,$$
$$\varphi_{23} = (\beta_3 - \beta_2) - k(R_3 - R_2)\,.$$

According to the above deduction, let the space between each two antennas on TOA be *24mrad* and the wavelength be *3mm*, the superposed electromagnetic fields on the receiving antenna aperture surface, whose size is 0.4m, are shown in Fig. 4, Fig. 4(a) for electric field intensity and Fig. 4(b) for phase. In the figure, “Array Simulation” denotes the result generated by TOA and “Theory” denotes the result generated by a Source Point (SP), which can be considered as the real electromagnetic field radiated from target seen as One-point in the space.

In Fig. 4(a), the electric field intensity of TOA is three times larger than which of SP. After normalization, the electric field intensity of TOA will be basically the same as which of SP. The error distribution of the electric field intensity is shown in Fig. 5(a), in which the average of error is -3.3×10^{-3} and the variance is 2.1×10^{-3}. The error distribution of the phase is shown in Fig. 5(b), in which the average of error is 4.82×10^{-5} and the variance is 2.63×10^{-2}.

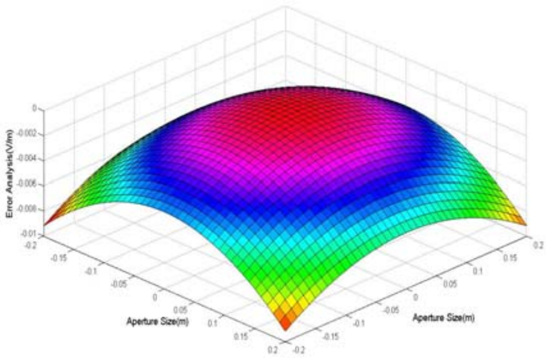

(a) Electric Filed Intensity

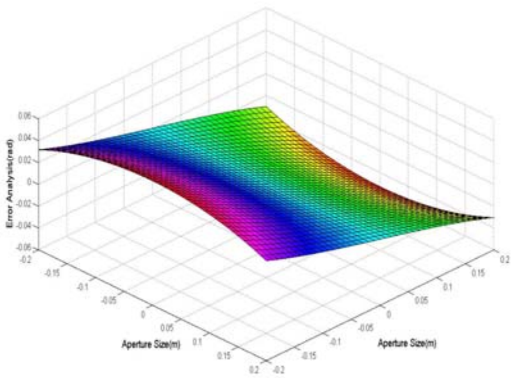

(b) Phase

Fig. 5 Error Distribution of TOA and SP

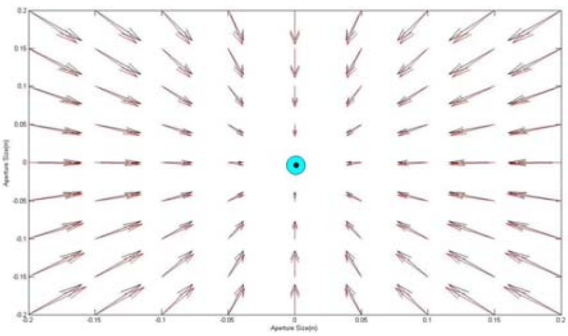

Fig. 6 Gradient and Normal of the Phases Wave-front

Because angular measurement of radar is based on the gradient direction of the phase wave-front formed by scattering electromagnetic waves on antenna aperture surface, Fig. 6 shows the direction of gradient and normal for phase wave-front when observing from target to seeker. In the figure, the trend of the black arrows and red arrows which denotes the gradient directions of SP and TOA respectively, are consistent with each other. Meanwhile, the normals of both are in the same direction that pointing at the target.

Thus, the electric field intensity and phase distribution simulated by TOA on the aperture of seeker are basically consistent with which of a SP generating. For the reason that One-point target can be well simulated by the TOA array[4], we employ it in our MMWSS in the experiment of high resolution seeker detection.

3.2 Simulation of Extended Target

Here we use two TOA arrays to simulate the extended target with two SC. Each TOA generates a SC. According to the derivation in the One-point target simulation, the synthetic electric field intensity on the seeker's aperture is $|E_k(x,y,z)|$ and the phase is $\beta_k(x,y,z)$ $(k=1,2)$. $|E_k(x,y,z)|$ and $\beta_k(x,y,z)$ follow equation (6) and (7). Thus the synthetic electric field intensity of two TOA is

$$E(x,y,z) = |E_1(x,y,z)|\exp[j\beta_1(x,y,z)] + |E_2(x,y,z)|\exp[j\beta_2(x,y,z)] \quad (8)$$

So

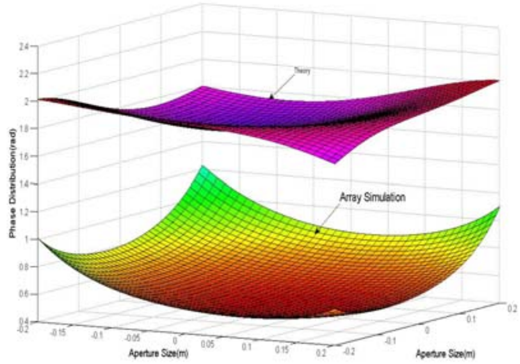

(b) Phase Distribution

Fig. 7 Electromagnetic Fields of TOA and Extended Target

$$|E(x,y,z)| = \sqrt{|E(x,y,z)|^2 + |E(x,y,z)|^2 + 2|E_1(x,y,z)||E_2(x,y,z)|\cos[\beta_1(x,y,z)-\beta_2(x,y,z)]} \quad (9)$$

$$\beta(x,y,z) = a\tan\frac{E_1(x,y,z)\sin\beta_1(x,y,z)+E_2(x,y,z)\sin\beta_2(x,y,z)}{E_1(x,y,z)\cos\beta_1(x,y,z)+E_2(x,y,z)\cos\beta_2(x,y,z)} \quad (10)$$

Based on the above inference, the two SC are separated from each other with *10mrad* in azimuth and *-10mrad* in elevation. The distribution of intensity and phase of the synthetic electric field are shown in Fig. 7. "Array Simulation" denotes the result generated by TOA and "Theory" denotes the result generated by extended target, which is the real electromagnetic field radiated from extended target with two SC in the space.

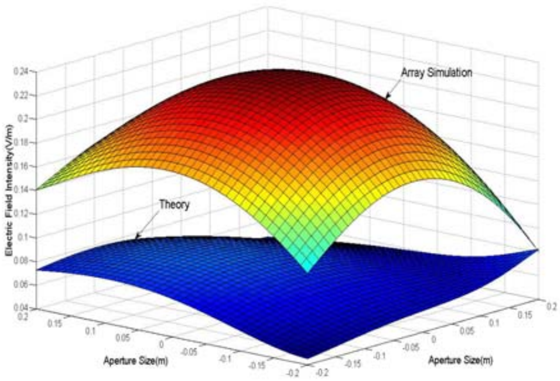

(a) Electric Field Intensity Distribution

The error distribution of electric field intensity and phase are shown in Fig. 8. The average error of the electric field intensity is -7×10^{-3}, twice as that of One-point. And the variance is 8.6×10^{-3}, 3 times greater than that of One-point. The average error of phase is -1.1537, up to 20000 times larger than that of One-point, and variance is 0.1539, almost 6 times large than that of One-point.

It is clearly in Fig. 9 that the gradient and normal of the Phase Wave-front for TOA and extended target are totally different. In that way, TOA array can not satisfy the precision in extended target simulation.

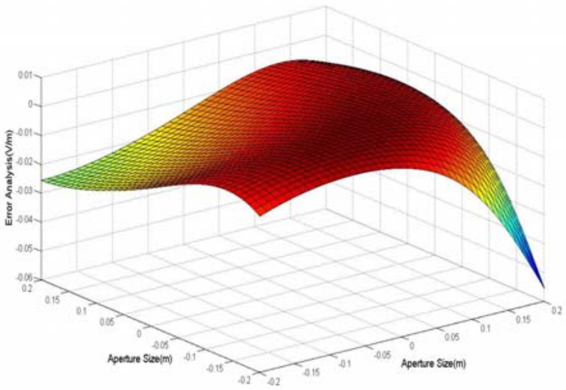

(a) Electric Filed Intensity

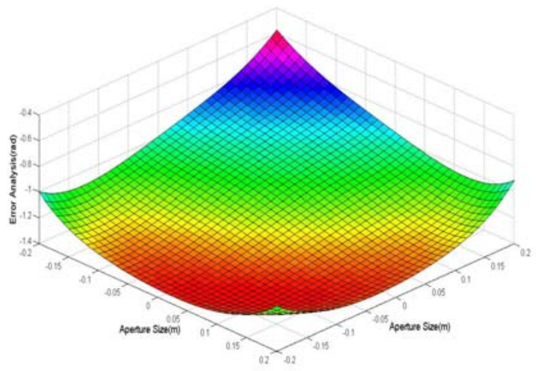

(b) Phase

Fig. 8 Error Distribution of TOA and Extended Target

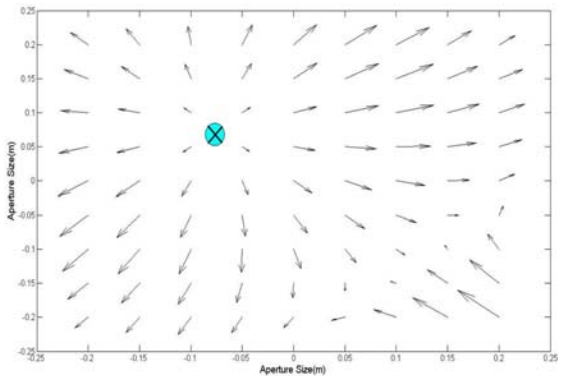

(a) Extended Target

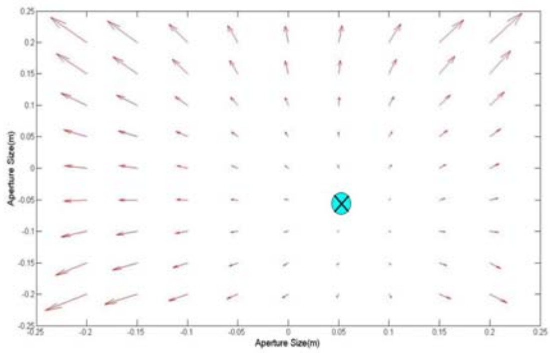

(b) TOA

Fig. 9 Gradient and Normal of the Phases Wave-front

In sum, the far-filed correction is absolutely necessary for extended target simulation to correct the synthetic electromagnetic fields generated by TOA, the processing of which is shown in Fig. 10.

4 Conclusion

This paper analyzes the target simulation in MMWSS with TOA array and shows that the far-field correction is quite necessary, because the TOA array acts ineffectively for extended target.

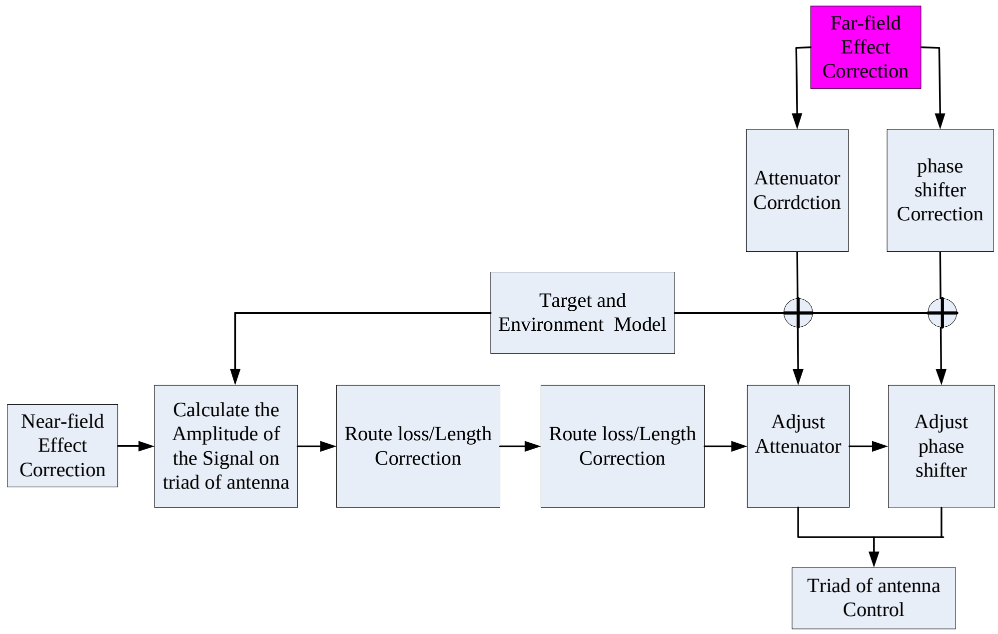

Fig. 10 Amplitude-phase Control Processing

5 Reference

[1] Xuguang LUO, Bin SHI, Ronghui SHEN, Congjun JIN, etc., Wide band MMW target HWIL Simulation System, Proceeding of Simulation Technology China, 2009, pp:241-249.

[2] Weimin LI; Yongfeng ZHU; Hongzhong ZHAO; Qiang Fu, The processing of target resolving for radar extended target detection, Proceeding of IEEE International Conference on Robotics, Intelligent Systems and Signal Processing, 2003, pp: 1256-1260

[3] Dean D. Howard, Radar Target Angular Scintillation in Tracking and Guidance Systems Based on Echo Signal Phase Front Distortion[C], Proceeding of the National Electronics Conference, 1959, Volume XV.

[4] C.B. Bishop, Error Analysis of Point Targets in HWIL simulation, Proceeding of the 1994 SCSC, 1994, pp:373-378.